THE JOURNAL OF BIOLOGICAL CHEMISTRY VOL. 287, NO. 6, pp. 3842–3849, February 3, 2012
Published in the U.S.A.

Exosome-associated Tau Is Secreted in Tauopathy Models and Is Selectively Phosphorylated in Cerebrospinal Fluid in Early Alzheimer Disease*[S]

Received for publication, June 28, 2011, and in revised form, November 2, 2011 Published, JBC Papers in Press, November 4, 2011, DOI 10.1074/jbc.M111.277061

Sudad Saman[‡], WonHee Kim[‡], Mario Raya[§], Yvonne Visnick[§] Suhad Miro[§], Sarmad Saman[§], Bruce Jackson[§], Ann C. McKee[¶‖], Victor E. Alvarez[¶‖], Norman C. Y. Lee[**], and Garth F. Hall[‡1]

*From the [‡]Department of Biological Sciences, University of Massachusetts, Lowell, Massachusetts 01854, the [§]MassBay Community College Science Department STEM Division, Wellesley Hills, Massachusetts 02481, the [¶]GRECC Unit, Veterans Affairs Medical Center, Bedford, Massachusetts 01730, the [‖]Departments of Neurology and Pathology, Boston University School of Medicine, Boston, Massachusetts 02215, and the **Chemical Instrumentation Center, Department of Chemistry, Boston University, Boston, Massachusetts 02215*

Background: Tau is secreted unconventionally, possibly explaining increased CSF phosphotau levels in early AD.
Results: M1C cells secrete selectively phosphorylated, exosomal tau. These characteristics in early AD CSF tau suggest that CSF tau is secreted, not shed from dead neurons.
Conclusion: Tau secretion occurs early and may explain lesion spreading in AD.
Significance: Secretion biomarkers may become revolutionary prospective AD diagnostics.

Recent demonstrations that the secretion, uptake, and interneuronal transfer of tau can be modulated by disease-associated tau modifications suggest that secretion may be an important element in tau-induced neurodegeneration. Here, we show that much of the tau secreted by M1C cells occurs via exosomal release, a widely characterized mechanism that mediates unconventional secretion of other aggregation-prone proteins (α-synuclein, prion protein, and β-amyloid) in neurodegenerative disease. Exosome-associated tau is also present in human CSF samples and is phosphorylated at Thr-181 (AT270), an established phosphotau biomarker for Alzheimer disease (AD), in both M1C cells and in CSF samples from patients with mild (Braak stage 3) AD. A preliminary analysis of proteins co-purified with tau in secreted exosomes identified several that are known to be involved in disease-associated tau misprocessing. Our results suggest that exosome-mediated secretion of phosphorylated tau may play a significant role in the abnormal processing of tau and in the genesis of elevated CSF tau in early AD.

Although it has generally been assumed that extracellular accumulation of abnormally processed tau protein in Alzheimer disease (AD)[2] is due to the passive release of tau from dead/dying neurons, recent demonstrations of active tau secretion and interneuronal tau transfer from our laboratory (1–3) and elsewhere (4–6) have suggested that antemortem tau secretion might participate in AD pathogenesis, possibly as part of the mechanism underlying transneuronal lesion spread (1, 6). The identification of a common unconventional secretion mechanism (exosome-mediated release) for other aggregation-prone proteins (*i.e.* α-synuclein, prion protein, β-amyloid) prominent in neurodegenerative disease pathogenesis (Refs. 7–9; for review see Refs. 10 and 11) prompted us to investigate the possibility that tau might also be secreted via this mechanism, because a common misprocessing pathway could account for synergistic interactions between these proteins in the pathogenesis of multiple neurodegenerative conditions (12–14). Here, we report that tau can be exported via an exosome-mediated mechanism in the M1C neuroblastoma tauopathy model (15), where it is enriched in a phosphotau biomarker for early AD (AT270) (16). We also report that the elevated CSF levels of AT270+ phosphotau seen in mild/moderate cases of sporadic AD relative to non-AD controls (17, 18) can be accounted for by a significant and selective enrichment of AT270+ tau in exosomal fractions of CSF relative to total CSF tau and that this is most marked in mild (Braak stage 3) (19) stages of AD.

EXPERIMENTAL PROCEDURES

Cells—We used M1C cells derived from human neuroblastoma (BE(2)-M17D) cells (kindly provided by Dr. Li Wen Ko of the Mayo Clinic College of Medicine, FL) to inducibly express wild-type human tau, with 4R0N (four MTBRs and zero N-terminal inserts) tau expression being induced by the TetOff expression system (TetOff). M1C cells were seeded in Dulbecco's modified Eagle's medium supplemented with 10% FBS, G418 (400 μg/ml), hygromycin (100 μg/ml), zeocin (100 μg/ml), and tetracycline (2,000 ng/ml). Tau expression was induced by reduction of tetracycline to 1 ng/ml for 6 days after which time M1C cells (comprising the cell lysate; Fig. 1) were lysed in Tris-NaCl (TN) buffer (50 mM Tris-HCl, pH 7.4, 150 mM NaCl, 1% Triton X-100, 10% glycerol, 2 mM EDTA, Com-

* This work was supported by the Boston University Alzheimer's Disease Center (BUADC), NIA grant P30 AG13846, a BUADC pilot grant (to G. F. H.), and the Department of Veterans Affairs.
[S] This article contains supplemental Fig. 1 and Table 1.
[1] To whom correspondence should be addressed: Dept. of Biological Sciences, University of Massachusetts, 198 Riverside St., Lowell, MA 01854. Tel.: 978-934-2893; E-mail: garth_hall@uml.edu.
[2] The abbreviations used are: AD, Alzheimer disease; CSF, cerebrospinal fluid; EP, exosome pellet; LSP, low speed pellet; MP, membrane pellet; MTBR, microtubule binding repeat; NFT, neurofibrillary tangle; 4R0N, exon 2,3 tau isoform with four MTBRs.

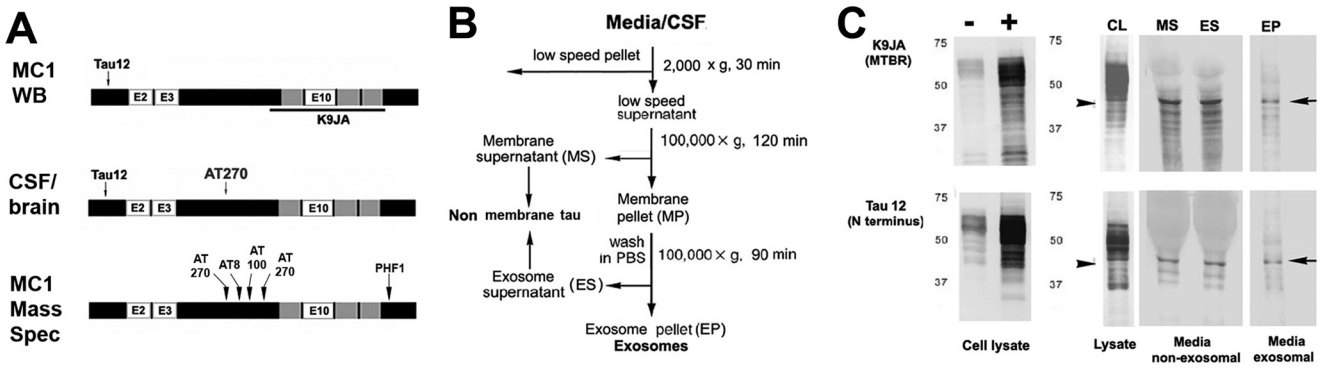

FIGURE 1. **Generation and characterization of exosomal fraction tau in M1C cells.** *A*, epitope locations of antibodies used in this study. Experimental results presented in this study are comparisons between mAbs marking all tau isoforms (*Tau12*) phosphorylated at the AT270 site (Thr-181). The polyclonal K9JA was also used in some M1C analyses to identify the MTBR region of tau (*e.g. C*, *top*). *B*, fractionation procedure used on M1C media and cell lysates and CSF/brain homogenate samples to obtain exosomes. After removal of the low speed cell debris pellet, the supernatant was then either analyzed directly (whole CSF or lysate) or then serially ultracentrifuged and washed to obtain non–membrane-associated (*MS*, *ES*) and membrane-associated fractions from M1C cell lysates and media fractions. LSPs were not removed from the raw samples used in Western blotting. An additional sucrose fractionation step (data not shown) was performed in all analyses involving human CSF and homogenates and in the preparation of all M1C fractions examined using mass spectrometry and immunoelectron microscopy (for details, see "Experimental Procedures"). *C*, antibodies to different parts of the tau molecule (*A*) were used to characterize exosomal tau (*EP*) *versus* nonexosomal secreted tau (*MS* and *ES*) purified using the protocol shown in *B*. Both nonexosomal (*i.e.* non–membrane-associated) and EP tau occur primarily of a near full size (40–45-kDa) fragment (*arrows*) fragment containing both the N terminus and the MTBR, plus a set of smaller cleavage products, presumably the result of intracellular turnover mechanisms prior to secretion, because the bands are also present in the cell lysate (*CL*). Note that the major band is similar to but somewhat larger than the 35-kDa AT270+ tau species identified in exosomal CSF fractions in AD (shown in Fig. 2*E*). Noninduced and induced cell lysates run on a separate gel are shown for comparison (*C*, *left lanes*).

plete EDTA-Ca^{2+}-Free mixture tablet (Roche Applied Science)). Cell lysates were cleared by centrifugation at 10,000 × *g* for 20 min.

Exosome Purification and Western Blot Analysis of M1C Medium and Lysates—A slightly modified version of the basic exosomal purification protocol of Théry *et al.* (20) was used to prepare exosomal fractions from M1C conditioned medium and lysate samples. Conditioned medium from the last 24 h of induction was collected from M1C cells expressing 4R0N tau and sequentially centrifuged at 2,000 × *g* for 10 min, and 10,000 × *g* for 30 min at 4 °C. To purify exosomes, the supernatant was then centrifuged at 100,000 × *g* for 90 min at 4 °C to obtain a membrane pellet (MP; Fig. 1*B*). This pellet was washed in cold PBS and centrifuged again at 100,000 × *g* for 90 min at 4 °C to remove any contaminating nonexosomal proteins. The supernatant (ES), with non–exosome-associated tau, was collected, and the pellet (EP), containing exosomes, was resuspended in 50 μl of PBS. Whole cell lysate/media samples and exosome fractions of these samples were analyzed by Western blotting. Electrophoresed samples were transferred to polyvinylidene difluoride membrane and incubated with the following primary antibodies: tau12 (1:10,000), K9JA (1:1,000; DAKO), anti-PDCD61P/Alix (1:500; Invitrogen), anti-flotillin 1 (1:1,000; Abcam), and anti-EEA1 (1:1,000; Abcam). Goat anti-mouse (1:10,000) or anti-rabbit (1:10,000) IgG, with or without alkaline phosphatase-conjugated second antibodies, were applied as second antibodies. Western blot images were obtained using a chemiluminescence (Pierce) or 5-bromo-4-chloro-3-indolyl phosphate/nitroblue tetrazolium substrate.

Preparation of CSF Exosome Fractions via Sucrose Gradient Fractionation—The additional sucrose fractionation step given by Théry *et al.* for "viscous bodily fluids" (supporting protocol 7) for preparing exosomes (20) was added to the basic protocol described above (20) for the isolation of CSF exosomal fractions. Membrane pellets isolated by ultracentifugation from CSF samples as described above were resuspended with 2 ml of isolation buffer and a linear sucrose gradient (2.0–0.25 M sucrose in 20 mM HEPES, pH 7.2) was layered on top of the exosome suspension. The sample was then centrifuged at 70,000 × *g* for 16 h at 4 °C and immunoblotted as described above or subjected to ELISA as described below. This approach was also used in some cases to identify and isolate specific populations of membranous vesicles (*i.e.* nuclei, mitochondria, Golgi, exosomes) from the MP (Fig. 1*B* and results not shown). A simpler version of this method directed at exosomes only was used to prepare exosomal fractions from membrane pellets of MC1 lysate and media fractions to be analyzed by EM and mass spectrometry.

Enzyme-linked Immunosorbent Assay of CSF Tau Samples—Direct ELISAs were done using the anti-phosphorylated tau mAb against phosphorylated Thr-181 (AT270) and an mAb capable of recognizing all tau isoforms (tau12) (see Figs. 1*A* and 3*A*). ELISA readings were converted to protein estimates using standard curves generated against optimized dilutions of each mAb. We used the ratios of tau phosphorylated at Thr-181 (AT270) to total tau (tau12) protein levels to characterize the phosphorylation state of CSF tau samples with a kit (KHO0631; Invitrogen) designed for ELISA quantitation of Thr-181 with modifications as described for use with mouse mAbs. All samples were diluted to a final concentration of 10 mg/ml protein in carbonate buffer. Wells of a PVC microtiter plate were coated with the diluted sample using the protocol provided with the kit. This was followed by addition of monoclonal antibodies AT270 and tau12 at dilutions of 1:1,500, 1:2,000, and 1:3,000, respectively. Optimal dilutions for each mAb were selected based on standard curves generated as described below. Goat anti-mouse IgG HRP secondary (ScC2005; Santa Cruz Biotechnology) was used as recommended at a concentration of 1:2,000. Revealing was done with a tetramethylbenzidine-based stabilized peroxidase substrate kit (KPL) on a Spectra Max M2

plate reader spectrophotometer (Molecular Devices). Standard curves were generated using purified antigen samples as follows. For AT270, standard dilutions of purified phosphotau Thr-181 supplied with the kit were used as directed. For tau12, purified recombinant tau381(4R0N) obtained from rPeptide were diluted serially and used to prepare three standard curves, with the curve yielding the greatest linearity in the picomole range being used for the calculation of sample protein concentration. For the correlation of AT270 distribution with Braak stage (see Fig. 3), we used the Innotest phosphotau assay kit (Innogenetics, Atlanta, GA), which employs the H7 mAb to capture CSF tau, which is then revealed using AT270. Assays were performed exactly as directed by the manufacturers' instructions.

CSF Samples and Low Speed Pellets from AD and Control Patients—CSF and brain samples used in this study were collected as part of the Boston University Alzheimer's Disease Center Brain Bank located at the Edith Nourse Rogers Memorial Veterans Hospital (Bedford, MA) following institutional IRB approval. The brains of all patients included were neuropathologically analyzed for limbic and isocortical neurofibrillary pathology and Braak-staged (19). Control (Braak stage 0–2, $n = 9$), mild AD (Braak stage 3–4, $n = 10$), and moderate AD (Braak stage 5, $n = 7$) groups had similar age profiles (77.6 ± 3.9, 81.6 ± 1.2, respectively) and postmortem intervals (11.3 ± 2.5, 14 ± 8, 14.2 ± 1.8 h, respectively). Because the goal of the study was to distinguish the exosomal contribution of total and AT270+ phosphotau specifically in AD, we included, as controls, brains with vascular lesions and/or Lewy bodies, as long as there was no neuropathological evidence of a tauopathy. We rejected samples from patients diagnosed with conditions associated with AD-like CSF tau levels or featuring ongoing pathogenesis involving the limbic and isocortices (*e.g.* multi-infarct, vascular (17), and Lewy body (18) dementias were included; corticobasal degeneration, Pick disease, and prion diseases were excluded). Samples containing blood or other visible impurities were rejected. All CSF samples (1–4 ml/subject) were kept frozen at −80 °C without freeze/thaw cycles after collection postmortem and were provided in polystyrene tubes. For all ELISA analyses, we subjected raw CSF samples to a standard low speed spin (2,000 × *g*, 30 min) and kept the supernatants for further processing and analysis. Low speed pellets from control (Braak stage 0), very mild (Braak stage 3), and severe (Braak stage 6) AD cases were photographed immediately after centrifugation and were assayed for tau content by direct ELISA (see Fig. 3*C*). Phosphatase inhibitor (20 μl/liter sample of Halt Phosphatase Inhibitor mixture, which was 2× the effective concentration given by the manufacturer) was added to all samples upon initial thawing.

Electron Microscopy—Pellets collected after the second 100,000 × *g* centrifugation step were fixed 20 min in 2% paraformaldehyde, loaded on Formvar/carbon-coated EM grids, and contrasted in 2% uranyl acetate, pH 7, and 2% methylcellulose/0.4% uranyl acetate, pH 4. Grids were postfixed 15 min in 1% glutaraldehyde for 5 min, washed 8 times with distilled water, contrasted, and embedded before examination using a CM 10 Twin Phillips electron microscope at 80 kV (Phillips Electronic Instruments, Rahway, NJ). Immunogold labeling of exosome preparations was accomplished by treating the Formvar grids with exosome sample prepared as described above, blocking with 1% BSA/5% normal goat serum followed by incubation with anti-ALIX/PDCD61P primary diluted 1:25 in blocking solution, followed by PBS rinse and incubation with 10 mM gold-labeled goat anti-mouse IgG secondary (Santa Cruz Biotechnology).

Mass Spectrometry—Samples from all fractions were diluted 1:1 with Laemmli sample buffer (Bio-Rad) containing 5% v/v 2-mercaptoethanol. Tris-HCl gels and Tris/glycine/SDS buffer were used for electrophoresis. Electrophoresis was performed first at a constant 90 V for 10 min and then at a constant 150 V until the dye front reached the end of the gel. A Bio-Rad Trans-Blot transfer cell and 40% Tris/glycine, 40% Tris/glycine/SDS, 20% methanol were used to transfer proteins to Bio-Rad Immun-Blot PVDF membranes at a constant 20 V overnight. Tryptic digests of peptides for mass spectrometry were performed using the In-Gel tryptic digest kit (Thermo Scientific). Samples of digested peptides from raw and exosomal fractions of M1C lysates and media were desalted and analyzed by MALDI mass spectroscopy in the positive mode at the Boston University, Chemical Instrumentation Center using standard reverse phase LC/MS (injection volume, 10 μl) Electrospray ionization on a Waters Qtof API US instrument from 100 to 8,000 *m*/*z*. The optimized conditions were found as follows: capillary, 3,000 kV; cone, 35; source temperature, 120 °C; and desolvation temperature, 350 °C. The gradient was 100% A (water + 0.1% formic Acid) to 100% B (acetonitrile + 0.1% formic acid) at 0.5 ml/min in 30 min. The column (Inertsil ODS-4, GL Sciences) used was a 250 × 4.6 mm with a particle size of 5 μm. Deconvolution was carried out by MaxEnt 1. Identification of proteins containing specific peptide sequences was accomplished by searching online data bases maintained on the ExPASy proteomics server using the peptide mass fingerprinting tool MASCOT (Matrix Science Ltd., London, UK). Only proteins with match ratios (based on Mascot data base searches) indicating a 95% or greater confidence in the identity of the specific protein listed were included. A subset of 65 of these proteins (supplemental Table 1) that was identified in 60% or more of the samples tested and enriched in secreted *versus* lysate exosome fractions was analyzed further (Fig. 2*A*). Semiquantitative analysis of protein enrichment (for both associated proteins and phosphotau peptides (Fig. 3*B*) was based on a comparison of peak heights between cell lysate and media-derived exosome fractions.

Data Analysis—A one-tailed Student's *t* test for unpaired samples was used to determine the significance of the 2-fold mean difference in AT270+ between control and AD samples, whereas a two-tailed *t* test for pairwise comparisons between linked data sets was used to determine whether AT270+ tau was significantly enriched in exosomal fractions compared with whole CSF samples in both control and AD patients. Fisher's exact test was used to test the significance of Braak staging on the distribution of AT270 tau between total CSF and exosomal fractions (see Fig. 3). Image processing of Western blots (Figs. 1*C* and 2, *B* and *E*) and EM micrographs (Fig. 2*C*) was minimal and performed as needed only for lettering and sizing using Adobe Photoshop according to JBC guidelines.

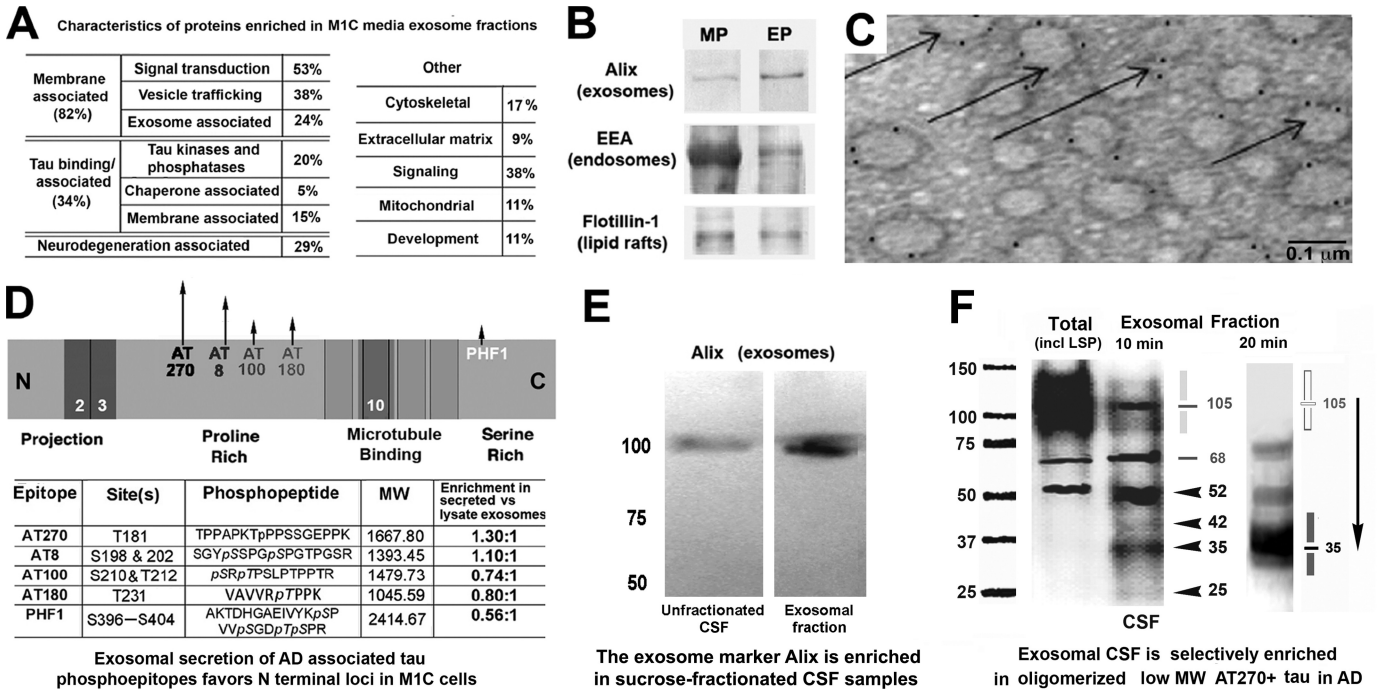

FIGURE 2. **Characteristics of exosome-associated tau in M1C cultures and human brain and CSF samples.** Secreted tau is associated with vesicular elements positive for exosomal markers and is enriched in exosome fractions of conditioned media samples from M1C cultures induced to overexpress a tau isoform lacking the exon 2 insert (4R0N) as determined by mass spectrometric (*A*) and Western blot (*B*) analysis. *A*, total of 237 proteins were identified in exosomal fractions of M1C cells induced to overexpress 4R0N tau. We identified 65 different proteins with which secreted tau was co-enriched using the Mascot peptide fingerprinting program (see "Experimental Procedures"). Of these, four classes of proteins were prominent. Most co-purifying proteins identified were intrinsic or membrane-associated proteins with signal transduction or vesicle trafficking functions. Such proteins are typically exosome-associated and include some (*e.g.* annexin 7, Alix) that are considered exosome "markers." Other co-enriched proteins included known tau-binding proteins that are affected in tauopathies (fyn kinase and the AD halllmark peptide β-amyloid 1–42). *B*, Western blots of endosome (EEA), exosome (Alix), and lipid raft membrane domains (flotillin 1) markers in exosomal (EP) and other membrane pellet-associated (MP) fractions from M1C samples are shown. Alix is enriched in the EP relative to the crude membrane pellet, whereas the early endosome antigen (*EEA*), a general endosome marker, is present in many cellular membranes. Flotillin 1 is a lipid raft marker present in trafficking vesicles, including exosomes. *C*, immunoelectron microscopy of an M1C exosome fraction shows colloidal gold decoration of the exosome marker protein Alix on 60–100-nm vesicles (*arrows*). *D*, relative enrichment of secreted phosphotau in exosomes (normalized to lysate exosomal tau) is illustrated in the schematic (*top*), with some sites (*e.g.* AT270, AT8) in the proline-rich domain being more prominent in secreted tau (*arrows*) than in lysate exosome fractions. Table (*bottom*) shows AD-associated phosphotau epitopes in exosomal fractions of M1C lysate and media samples as determined using mass spectrometry. The presence of specific phosphoepitopes in was identified using the peptides shown for each epitope. *E*, immunoblot of unfractionated (*center*) and an exosome fraction (*right*) from an early AD (Braak stage 4) CSF sample shows the presence of the exosome marker Alix in unfractionated CSF and its enrichment in an exosomal fraction of the same sample isolated by ultracentrifugation followed by sucrose fractionation (see "Experimental Procedures"). *F*, Western blots of CSF samples from a moderate AD case (Braak stage 5) are shown as immunolabeled with the mAb AT270 (Thr(P)-181). *Left*, raw unfractionated (*left lane*) and exosomal fraction (*right lane*) for CSF samples immunoblotted with AT270 show enrichment for low molecular mass tau species in the exosomal fraction CSF relative to unfractionated CSF (*carets*). Most high molecular mass tau species are reduced in exosomes relative to the total sample with the notable exception of a single high molecular mass band at 105 kDa (*line*, *shading*). *Right*, increasing the denaturation stringency of CSF exosome fractions from 10-min heating at 90 °C in 1× SDS buffer (*left* and *center lanes*) to 20 min in 2× SDS buffer at 90 °C (*right lane*) completely abolishes all high molecular mass (presumably multimeric) tau bands above the iconic 68-kDa phosphotau band (Ala-68) characteristic of AD (32, 33). Note that the more stringent boiling regime selectively increases the mobility of high molecular mass tau 3-fold (compare *carets* with *shading*). The sharp 105-kDa band is completely abolished, the 68-kDa and 52-kDa bands reduced, and the exosomally enriched species at 35 kDa augmented by stringent (20 min) boiling, suggesting that a significant proportion of exosomally secreted tau exists as dimeric (52, 68 kDa) and (especially) trimeric AT270 + 35 kDa tau fragments (*shading* at *right*).

RESULTS

Secreted Tau in M1C Cells Co-purifies with Exosomal Membrane Fraction and with Exosome-associated Proteins—We extended earlier studies of 4R0N tau secretion from M1C neuroblastoma cells (2) by investigating the possibility that the tau found in M1C conditioned media after TetOff induction (15) is membrane-associated, because nonconstitutive unconventional protein secretion pathways typically involve the release of proteins associated with vesicles (21). M1C media samples were collected from cultures after 24 h of 4R0N tau induction and subjected to sequential high speed centrifugations to isolate exosomal, nonexosomal membrane and nonmembrane fractions (Fig. 1*B*) from M1C supernatants and cell lysates, which were then analyzed by SDS-PAGE and immunoblotting for the presence of tau. The identity of each fraction was verified by immunoblotting of crude MPs, nonexosomal supernatants (ES, MS), and exosome pellet (EP) fractions with antibodies against endosome (EEA1), lipid raft (flotillin 1), and exosome (PDCD61P/Alix) markers (Fig. 2*B*). Secreted tau was present in all three fractions as a strong 45-kDa band that was immunopositive for N terminus (tau12) and MTBR-specific (K9JA) antibodies, suggesting that it had been C-terminal-truncated but was otherwise intact (2). Immunoelectron microscopic analysis of tau-containing exosome fractions showed vesicular elements of uniform appearance with the expected size (~40–100 nm) and morphology of exosomes (21–23), which were specifically identified by mAbs to the exosome marker PDCD61P (also known as Alix) (Fig. 2*C*).

Mass spectrometric analysis of tau-containing exosome fractions secreted from M1C cells identified a large number of asso-

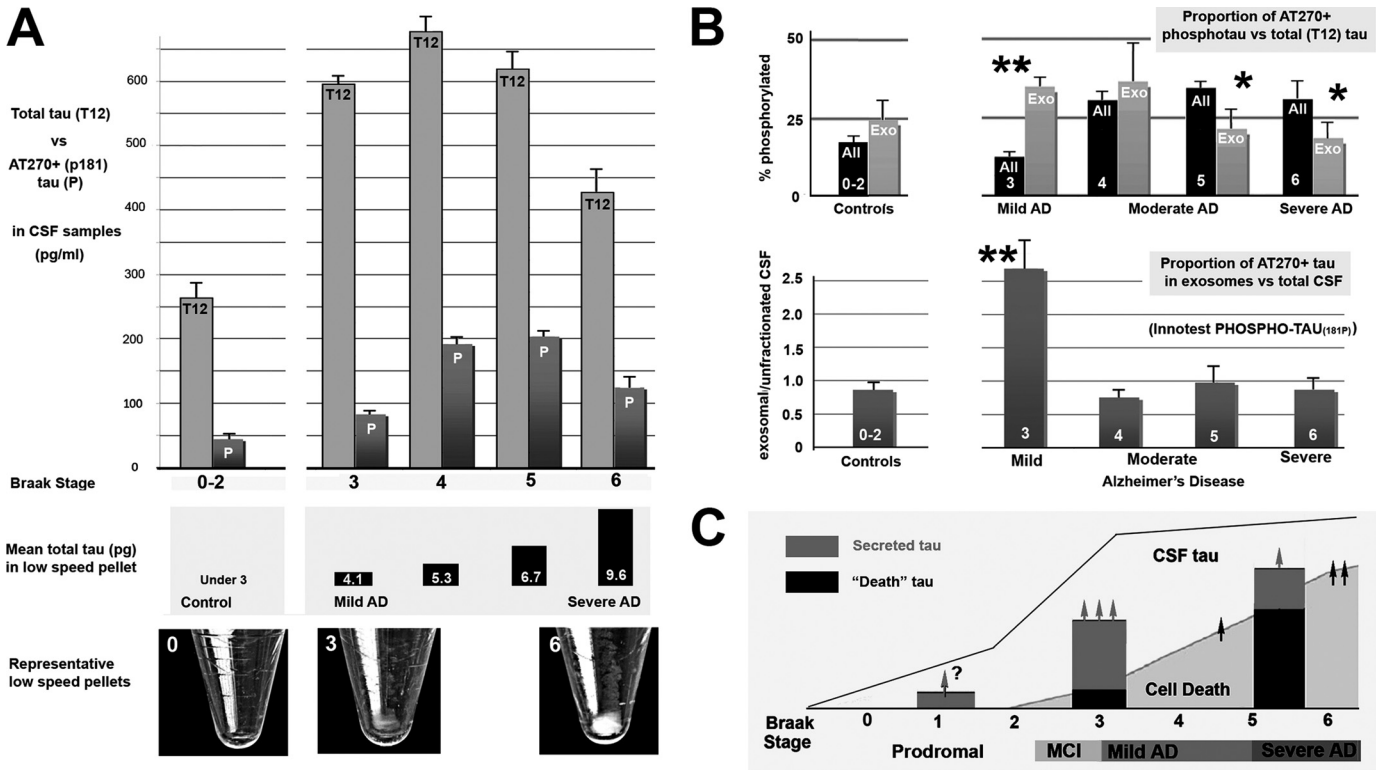

FIGURE 3. **Increased exosomal AT270 in CSF is specific to early AD and is not associated with large scale neuron loss.** The distribution of phosphotau Thr-181 (AT270+ tau) between exosomal and unfractionated CSF samples changes characteristically with increasing severity of AD as determined by Braak stage. *A*, *top*, gross CSF levels of total (tau12) and AT270+ phosphorylated tau (*P*) levels in control patients with mild, non-AD dementia (*left*) and increasingly severe Braak stages of AD (*right*) were compared using ELISA-based analysis. Samples were analyzed after the removal of the LSP, consisting of dead cells/cell debris. CSF total tau and phosphotau levels rise significantly above control values only with mild-moderate (stage 4) AD cases and remain somewhat elevated relative to controls in severe AD. In contrast, the tau content (*center*) and gross size of LSPs (*images*, *bottom*) increase markedly only in moderate-severe AD. *B*, analysis of the distribution and phosphorylation state at Thr-181 (AT270) in unfractionated (*black*) and exosome (*gray*) fractions of CSF tau in CSF samples from 9 control and 21 AD patients sorted according to the Braak stage of neurofibrillary degeneration determined at the time of death. Each sample was characterized using two different analyses: (i) the percentage of phosphorylated *versus* total tau (%P) was determined using direct ELISA as described under "Experimental Procedures" (*top*), and (ii) the proportion AT270+ tau in exosomal fractions relative to unfractionated CSF was determined using the Innotest phosphotau kit (*bottom*). The increase in %P with AD onset (Braak stage 3) occurs as a marked spike in %P in the exosomal fraction (*double asterisks*, *top*), but not in unfractionated samples, which only show significant increases above either controls or exosomal fractions beginning at stage 4 (mild/moderate AD). The %P in exosomal tau declined progressively with increasing disease severity and was thus inversely related with the increasing %P of the total sample, which was significantly more phosphorylated than the exosomal fraction by stages 5 and 6 (*single asterisks*). Upon retest with the Innotest kit, the significant spike in mild (stage 3) AD relative to both controls and later stages of AD remained. *Bars* indicate S.E. in both *A* and *B*. Significant differences (Fisher's exact test) were found between controls and stage 3–5 AD in *A* ($p < 0.02$ for 3–5) and between the proportion of AT270 tau in the exosomal fraction in stage 3 *versus* controls ($p < 0.002$) and *versus* later stages of AD ($p < 0.001$). *C*, proposed timeline of events relevant to the generation of CSF tau in AD is based on the results of this study. We hypothesize that in normal aging, only a small proportion of vulnerable neurons in certain parts of the CNS (*e.g.* temporal limbic cortices) secrete tau, which could account for the age-associated increase CSF tau (*arrow*, *question mark*). In the earliest clinical stages of AD (Braak stage 3, including mild cognitive impairment (*MCI*), tau misprocessing becomes widespread, leading to significant secretion of AT270+ tau (*gray* bars) to the CSF, both from temporal limbic neurons as NFTs form and probably also from much larger neocortical areas in advance of NFT formation. Note that the neocortex does not become a major site of neuronal death until later stages of AD. Secreted tau becomes disassociated from exosomes via proteolytic degradation and moves out of the exosomal fraction over time (*gray arrows*). Large scale NFT formation and neuron loss begin to occur with the onset of "isocortical AD" at Braak stage 5 (26). This significantly increases the size of the LSP in stage 6 patients relative to stage 3 (*A*, *bottom*, $p < 0.01$) and may augment to some extent the level of phosphotau in the CSF (*arrow* at *right*), but does not offset the reduction in the number of "pretangle" neurons available to secrete tau by stage 6.

ciated proteins (24), most of which are typical for exosome preparations from various tissues and bodily fluids (7–9, 21–25, listed in supplemental Fig. 1). Although a detailed analysis of these proteins and their relationship to tau secretion is beyond the scope of this report, we performed a preliminary categorization of 65 proteins that were enriched in media exosome fractions relative to lysate fractions (Fig. 2*A*). The majority of these (82%) were membrane proteins or membrane-associated proteins involved in signal transduction and vesicle trafficking, including the widely cited markers of exosomes flotillin 1 and Alix (Fig. 2*B*). A large minority (34%) were proteins that have been reported to interact specifically with tau in ways that could favor its oligomerization, inclusion in exosomes, and ultimately its secretion (26), primarily via the phosphorylation of sites associated with tau oligomerization and toxicity (27–29; for review, see Refs. 30, 31). These proteins included the nonreceptor tyrosine kinase fyn (27, 28) and β-amyloid peptide 1–42 (29).

Exosomal Fractions of Conditioned Media Samples from M1C Are Enriched in Phosphotau Species Associated with Neurodegeneration—We used mass spectrometry to identify specific tau peptides (N-terminal, proline-rich, and MTBR regions) in both cell lysate and media exosomal fractions, confirming earlier work in this system based on Western blot analysis (1, 2). In particular, we found prominent peaks in exosome-associated secreted tau samples that were specific for tau phosphoepitopes (AT180, AT100, AT270, AT8, and PHF1) associated with AD. (Fig. 2*D*). Quantitative comparisons

between peaks representing specific phosphotau epitopes in exosome fractions from media and cell lysate samples showed that phosphorylated sites in the proline-rich domain of tau (AT270, AT8, AT100, and AT180) were most strongly enriched in secreted tau (Fig. 2*D*). Interestingly, AT270 (Thr(P)-181), the site most enriched in secreted (exosomal) tau, is also an established biomarker for the elevated tau seen in early AD and is used in CSF-based diagnostics for AD (16).

CSF Exosomal Fractions from AD Patients Contain Multimeric AT270+ Tau Species—To test directly the possible link between exosome-associated tau secretion and AD, we used Western blotting to determine whether the enrichment of AT270 tau seen in exosomally secreted tau fractions from M1C cultures was also present in similarly isolated fractions of CSF from mild (Braak stage 3) and established AD (Braak stage 5) cases (note that a sucrose fractionation step was added to the fractionation protocol for isolating CSF exosomes; see "Experimental Procedures"). We found that such fractions were enriched in Alix (Fig. 2*E*) and strongly positive for AT270+ tau (Fig. 2*F*). AT270+ tau was localized to a few major bands (35, 52, and 68 kDa), one of which (68 kDa) is characteristic of NFT tau in AD (32–34). Prominent higher molecular mass (80–150 kDa) bands in both unfractionated and exosomal fractions of CSF samples were 100% sensitive to high stringency denaturation (20-min heating in 2× SDS at 90 °C). Because tau is resistant to heat-induced precipitation (35), this indicates that the high molecular mass bands were due to noncovalent association with other proteins, most likely tau itself, because tau readily forms low level oligomers when associated with microtubules (36) and with membrane constituents such as fatty acids (37). In exosomal fractions, most AT270+ high molecular mass tau was concentrated in a strong, well defined band at around 105 kDa instead of the broad band between 80 and 150 kDa, which reduced to a very strong band at 35 kDa plus a widening of the 52-kDa band with stringent denaturation (Fig. 2*F*). This result thus strongly suggests that a large part of the exosomal AT270+ tau is in fact the 35-kDa tau species that has dimerized (70 kDa) and especially trimerized (105 kDa). The range of sizes associated with the total CSF sample between 80- and 150-kDa apparent molecular mass might contain variously cleaved tau oligomers associated with NFTs (38), especially because no initial low speed spin to remove cellular tau that had been shed into the CSF from dead neurons was performed with this experiment.

Elevated Phosphotau in AD CSF Samples versus Non-AD Controls Is Specific to Exosomes—To investigate the possibility that exosome-mediated tau secretion is involved in the production of the elevated CSF tau typically found in AD, we isolated exosomal fractions from CSF samples taken postmortem from 24 (Braak stage 3–6) AD cases and 9 age-matched non-AD (Braak stage 0–2) controls (see "Experimental Procedures") and measured the relative levels of AT270+ phosphotau and compared them with a total tau marker (tau12) in both exosome fractions and in the whole CSF sample. Direct ELISAs showed that overall CSF levels of both total tau and AT270 were very significantly elevated ($p \ll 0.001$, Student's t test for unpaired samples) over controls in the 17 (Braak stage 3–5) AD cases (Fig. 3*A*). Although the overall proportion of tau in the exosomal fraction relative to whole CSF was not significantly different between the control and AD groups, the proportion of phosphotau in the exosomal fraction was significantly higher ($p = 0.04$, Student's t test for unpaired samples) in the mild/moderate AD group than in controls. This was accompanied by a highly significant enrichment of phosphotau in the exosomal sample relative to whole CSF in the AD group ($p = 0.002$, two-tailed t test for paired samples). Both total and phosphotau CSF tau levels were somewhat reduced in severe AD cases (Braak stage 6) that we examined so that their elevation above the non-AD controls was only marginal ($p < 0.1$).

Exosomal AT270 Levels Are Transiently Elevated before the Onset of Widespread Neuron Death in AD—To test the widespread assumption that CSF tau (particularly CSF phosphotau) is due to antecedent neuron death, we conducted a more detailed study of the proportion of AT270+ phosphotau in the exosomal fraction relative to total CSF tau with the progression of AD in samples from patients who exhibited mild (Braak stage 3–4), moderate (Braak stage 5), and severe (Braak stage 6) neurofibrillary changes diagnostic of AD. We compared total tau and phosphotau data from direct ELISA analyses with the standardized clinical CSF assay for Thr(P)-181 phosphotau (the Innotest PHOSPHO-TAU$_{(181P)}$ ELISA kit) both to increase the sensitivity of our results and to facilitate their comparison with those from other CSF tau studies. We found that both methods showed marked highly significant initial increases of phosphotau in exosomal (but not total) tau fractions in the earliest (Braak stage 3) AD cases (Fig. 3*B*). The proportion of phosphotau in exosomes decreased with AD severity as the relative levels of phosphotau in the total sample increased, suggesting that exosome fraction tau might become progressively disassociated from exosomes as the disease progresses. The Innotest "capture" ELISA yielded levels of total CSF AT270+ tau that were very similar to the results obtained using the direct ELISA described above (Fig. 3*B*, compare *top* and *bottom graphs*). Again, most of the proportional elevation of AT270+ tau in exosomal CSF fractions in the AD patients was localized to patients that exhibited Braak stage 3 neurofibrillary pathology at the time of death (Fig. 3*B*) and returned to near control levels in samples from more severe AD cases. This result is consistent with a major role for active tau secretion in the genesis of CSF phosphotau in the earliest stages of AD and is in conflict with the hypothesis that high CSF tau levels in early AD are due to neuron death. This is corroborated by the relative size of the LSPs, which are a direct indication of the extent of neuron death, in many of the analyzed samples) spun down from control and AD patients (control, stage 3, and stage 6 samples are shown in Fig. 3*C*, *bottom*). We found that only stage 5–6 samples generated large pellets with high tau content, a pattern that is consistent with the neuropathological literature (39) but not at all correlated with the early elevation of CSF tau and phosphotau levels typically found in AD.

DISCUSSION

We show that tau secretion can occur via an exosome-mediated mechanism from M1C cells and that exosome-associated tau is a major component of the CSF tau seen in early AD patients. Exosomally released tau consists predominantly of a

35–40-kDa tau species that is (i) phosphorylated at sites that become phosphorylated in disease-associated mechanisms of tau misprocessing and (ii) exhibits characteristics (*i.e.* apparent low level oligomerization) that are associated with toxicity (40) and are involved in neurodegeneration and possibly interneuronal tau transfer (1–3, 5, 6, 26). Exosomal tau is associated both with typical exosomal proteins and with proteins involved in tau misprocessing and AD pathogenesis, such as β-amyloid, presenilins, and fyn kinase (Fig. 2*D*; see complete list in supplemental Table 1). We also show that exosome-associated tau phosphorylated at Thr-181 (AT270+ tau) is present in CSF samples from human AD patients and age-matched controls, where it was significantly enriched relative to total tau markers in exosomal fractions in very early AD patients relative to the enrichment seen in total CSF samples. This pattern was specific to early AD, being marked in patients with Braak stage 3 neurofibrillary pathology but progressively less so in later stages of AD and was absent from non-AD controls diagnosed with other dementing conditions (mainly vascular or Lewy body disease). These findings collectively suggest that that the initial elevation of phosphotau levels in AD is not associated with passive, nonspecific tau release consequent to neuron death, since only a small proportion of the brain is involved in neurofibrillary degeneration at this stage (39) and the later stages (Braak 5–6) of AD, in which neurons are lost in large numbers (Fig. 3*C*), are associated with exosomal AT270 levels similar to those of non-AD control patients. In tau-overexpressing M1C cells, exosomally secreted tau consists of a large (~40 kDa) tau species that contains both the MTBR and the N terminus, which is consistent with previously identified characteristics associated with tau secretion (1–3), toxicity (4), and uptake (1, 5), and resembles some of the CSF tau species found in AD (41) models (34) and non-AD tauopathies (42, 43). We also show that AT270 tau is selectively enriched in exosomal fractions from CSF relative to brain homogenates and that high molecular mass tau species in CSF exosomal fractions are very likely noncovalent oligomers of a 35-kDa phosphotau species that appears identical to the major AT270+ tau species associated with cognitive deficits and neurodegeneration in the rat tauopathy model (34). This tau fragment is selectively and strongly enriched in exosomal CSF (Fig. 2*E*). These findings thus identify a specific vesicle-trafficking pathway involved in tau secretion and constitute the first evidence that active tau secretion in human patients may be relevant to the genesis of elevated phosphorylated CSF tau in the early stages of AD. Moreover, tau secretion is potentiated by the same modifications that drive neurofibrillary degeneration (*i.e.* dissociation from microtubules, hyperphosphorylation of key serines and tyrosine residues, oligomerization) in AD, making potential tau secretion biomarkers (*e.g.* exosomal fraction tau, tau enriched in 0N isoforms (2) prime candidates for development as prospective AD diagnostics.

Although tau secretion and uptake by adjacent neurons *in situ* were identified a number of years ago in a tauopathy model with cell autonomous tau expression (44, 45), they have been characterized only recently in cell culture tauopathy models (1–3, 5). Tau secretion and uptake have so far been identified inferentially in murine transgenic models (6) but have not yet been directly demonstrated due to the difficulty of identifying the cellular origin of extracellular tau in such models. This difficulty, plus the lack of any secretion-associated motifs on tau, has fostered the assumption that tau secretion only occurs in association with nonphysiological tau overexpression and is thus irrelevant to tau pathobiology. However, recent demonstrations of high efficacy and specificity of tau secretion, toxicity, uptake, and interneuronal transfer in various tauopathy models (1–6) and that these events and characteristics are modulated by disease-relevant tau alterations such as phosphorylation (3, 27–31), cleavage (34, 38), and oligomerization (26, 37, 46, 47) suggest that secretion may play a significant role in tau-associated neurodegeneration. The involvement of tau secretion in the genesis of increased CSF tau levels in the earliest stages of AD may therefore mark a significant change in our overall view of AD pathogenesis, both because of the new insights that it provides into disease-associated mechanisms of tau misprocessing and because of the potential clinical importance of tau secretion biomarkers for CSF-based AD diagnostics. Exosomal secretion mechanisms have now been sufficiently characterized to offer clues to new avenues of research into how tau misprocessing and cytopathogenesis may be connected. For example, we identified specific proteins (*e.g.* fyn kinase, β-amyloid, presenilin) in association with exosomally secreted tau that play disease-related roles in protein phosphorylation (27–31), endocytosis (48), oligomerization (26, 36), and the disruption of protein turnover mechanisms (49, 50), all of which are characteristic of tau pathobiology and any of which could plausibly link exosome-mediated tau secretion with other aspects of tau-induced neurodegeneration. Exosome-mediated tau secretion in early AD is particularly interesting in light of recent findings that other aggregation-prone proteins involved in neurodegeneration (*e.g.* β-amyloid, α-synuclein, and prion protein) are secreted via an exosomal mechanism (7–9), because each of these proteins interacts with tau under neuropathogenic circumstances with the effect of exacerbating the oligomerization and neurotoxicity of the proteins involved (10). The presence of tau in the same cellular compartment as these other proteins in multiple neurodegenerative conditions thus suggests a plausible mechanism for this interaction that could account for the neuropathological synergy between AD and other neurodegenerative diseases at the cellular level (11).

Acknowledgments—We acknowledge the use of resources and facilities at the Edith Nourse Rogers Memorial Veterans Hospital.

REFERENCES

1. Kim, W., Lee, S., Jung, C., Ahmed, A., Lee, G., and Hall, G. F. (2010) *J. Alzheimers Dis.* **19,** 647–664
2. Kim, W., Lee, S., and Hall, G. F. (2010) *FEBS Lett.* **584,** 3085–3088
3. Lee, S., Kim, W., Li, Z., and Hall, G. F. (2012) *Int. J. Alz Dis.*, in press
4. Gómez-Ramos, A., Díaz-Hernández, M., Cuadros, R., Hernández, F., and Avila, J. (2006) *FEBS Lett.* **580,** 4842–4850
5. Frost, B., Jacks, R. L., and Diamond, M. I. (2009) *J. Biol. Chem.* **284,** 12845–12852
6. Clavaguera, F., Bolmont, T., Crowther, R. A., Abramowski, D., Frank, S., Probst, A., Fraser, G., Stalder, A. K., Beibel, M., Staufenbiel, M., Jucker, M., Goedert, M., and Tolnay, M. (2009) *Nat. Cell Biol.* **11,** 909–913
7. Rajendran, L., Honsho, M., Zahn, T. R., Keller, P., Geiger, K. D., Verkade,

P., and Simons, K. (2006) *Proc. Natl. Acad. Sci. U.S.A.* **103,** 11172–11177
8. Emmanouilidou, E., Melachroinou, K., Roumeliotis, T., Garbis, S. D., Ntzouni, M., Margaritis, L. H., Stefanis, L., and Vekrellis, K. (2010) *J. Neurosci.* **30,** 6838–6851
9. Fevrier, B., Vilette, D., Archer, F., Loew, D., Faigle, W., Vidal, M., Laude, H., and Raposo, G. (2004) *Proc. Natl. Acad. Sci. U.S.A.* **101,** 9683–9688
10. Cushman, M., Johnson, B. S., King, O. D., Gitler, A. D., and Shorter, J. (2010) *J. Cell Sci.* **123,** 1191–1201
11. Hall, G. F. (2011) in *Neurodegenerative Diseases–Processes, Prevention, Protection and Monitoring* (Chang, R. C.-C., ed) pp. 1–32, InTech, Rijeka, Croatia
12. Clinton, L. K., Blurton-Jones, M., Myczek, K., Trojanowski, J. Q., and LaFerla, F. M. (2010) *J. Neurosci.* **30,** 7281–7289
13. Gadad, B. S., Britton, G. B., and Rao, K. S. (2011) *J. Alzheimers Dis.* **24,** 223–232
14. Sharples, R. A., Vella, L. J., Nisbet, R. M., Naylor, R., Perez, K., Barnham, K. J., Masters, C. L., and Hill, A. F. (2008) *FASEB J.* **22,** 1469–1478
15. Ko, L. W., Rush, T., Sahara, N., Kersh, J. S., Easson, C., Deture, M., Lin, W. L., Connor, Y. D., and Yen, S. H. (2004) *J. Alzheimers Dis.* **6,** 605–622
16. Vanderstichele, H., De Vreese, K., Blennow, K., Andreasen, N., Sindic, C., Ivanoiu, A., Hampel, H., Bürger, K., Parnetti, L., Lanari, A., Padovani, A., DiLuca, M., Bläser, M., Olsson, A. O., Pottel, H., Hulstaert, F., and Vanmechelen, E. (2006) *Clin. Chem. Lab. Med.* **44,** 1472–1480
17. Arai, H., Satoh-Nakagawa, T., Higuchi, M., Morikawa, Y., Miura, M., Kawakami, H., Seki, H., Takase, S., and Sasaki, H. (1998) *Neurosci. Lett.* **256,** 174–176
18. Parnetti, L., Lanari, A., Amici, S., Gallai, V., Vanmechelen, E., and Hulstaert, F. (2001) *Neurol. Sci.* **22,** 77–78
19. Braak, H., and Braak, E. (1991) *Acta Neuropathol.* **82,** 239–259
20. Théry, C., Clayton, A., Amigorena, S., and Raposo, G. (2006) *Curr. Protocols Cell Biol.* Suppl. 30, 3.22.1–3.22.29
21. Nickel, W. (2005) *Traffic* **6,** 607–614
22. Simpson, R. J., Lim, J. W., Moritz, R. L., and Mathivanan, S. (2009) *Expert Rev. Proteomics* **6,** 267–283
23. Mathivanan, S., and Simpson, R. J. (2009) *Proteomics* **9,** 4997–5000
24. Pan, S., Aebersold, R., Chen, R., Rush, J., Goodlett, D. R., McIntosh, M. W., Zhang, J., and Brentnall, T. A. (2009) *J. Proteome Res.* **8,** 787–797
25. Harrington, M. G., Fonteh, A. N., Oborina, E., Liao, P., Cowan, R. P., McComb, G., Chavez, J. N., Rush, J., Biringer, R. G., and Hühmer, A. F. (2009) *Cerebrospinal Fluid Res.* **6,** 10
26. Fang, Y., Wu, N., Gan, X., Yan, W., Morrell, J. C., and Gould, S. J. (2007) *PLoS Biol.* **5,** e158
27. Lee, G., Newman, S. T., Gard, D. L., Band, H., and Panchamoorthy, G. (1998) *J. Cell Sci.* **111,** 3167–3177
28. Vega, I. E., Cui, L., Propst, J. A., Hutton, M. L., Lee, G., and Yen, S. H. (2005) *Brain Res. Mol. Brain Res.* **138,** 135–144
29. Busciglio, J., Lorenzo, A., Yeh, J., Yankner, B. A. (1995) *Neuron* **14,** 879–888
30. Stoothoff, W. H., and Johnson, G. V. (2005) *Biochim. Biophys. Acta* **1739,** 280–297
31. Wang, J. Z., Grundke-Iqbal, I., and Iqbal, K. (2007) *Eur. J. Neurosci.* **25,** 59–68
32. Lee, V. M., Balin, B. J., Otvos, L., Jr., and Trojanowski, J. Q. (1991) *Science* **251,** 675–678
33. Buée, L., and Delacourte, A. (1999) *Brain Pathol.* **9,** 681–693
34. Zilka, N., Korenova, M., Kovacech, B., Iqbal, K., and Novak, M. (2010) *Acta Neuropathol.* **119,** 679–687
35. Weingarten, M. D., Lockwood, A. H., Hwo, S. Y., and Kirschner, M. W. (1975) *Proc. Natl. Acad. Sci. U.S.A.* **72,** 1858–1862
36. Makrides, V., Shen, T. E., Bhatia, R., Smith, B. L., Thimm, J., Lal, R., and Feinstein, S. C. (2003) *J. Biol. Chem.* **278,** 33298–33304
37. Chirita, C. N., Necula, M., and Kuret, J. (2003) *J. Biol. Chem.* **278,** 25644–25650
38. Guillozet-Bongaarts, A. L., Garcia-Sierra, F., Reynolds, M. R., Horowitz, P. M., Fu, Y., Wang, T., Cahill, M. E., Bigio, E. H., Berry, R. W., and Binder, L. I. (2005) *Neurobiol. Aging* **26,** 1015–1022
39. Braak, H., Alafuzoff I., Arzberger, T., Kretzschmar, H., and Del Tredici, K. (2006) *Acta Neuropathol.* **112**, 389–404
40. Berger, Z., Roder, H., Hanna, A., Carlson, A., Rangachari, V., Yue, M., Wszolek, Z., Ashe, K., Knight, J., Dickson, D., Andorfer, C., Rosenberry, T. L., Lewis, J., Hutton, M., and Janus, C. (2007) *J. Neurosci.* **27,** 3650–3662
41. Johnson, G. V., Seubert, P., Cox, T. M., Motter, R., Brown, J. P., and Galasko, D. (1997) *J. Neurochem.* **68,** 430–433
42. Urakami, K., Wada, K., Arai, H., Sasaki, H., Kanai, M., Shoji, M., Ishizu, H., Kashihara, K., Yamamoto, M., Tsuchiya-Ikemoto, K., Morimatsu, M., Takashima, H., Nakagawa, M., Kurokawa, K., Maruyama, H., Kaseda, Y., Nakamura, S., Hasegawa, K., Oono, H., Hikasa, C., Ikeda, K., Yamagata, K., Wakutani, Y., Takeshima, T., and Nakashima, K. (2001) *J. Neurol. Sci.* **183,** 95–98
43. Borroni, B., Gardoni, F., Parnetti, L., Magno, L., Malinverno, M., Saggese, E., Calabresi, P., Spillantini, M. G., Padovani, A., and Di Luca, M. (2009) *Neurobiol. Aging* **30,** 34–40
44. Hall, G. F., Lee, V. M., Lee, G., and Yao, J. (2001) *Am. J. Pathol.* **158,** 235–246
45. Hall, G. F., Lee, S., and Yao, J. (2002) *J. Mol. Neurosci.* **19,** 253–260
46. Sahara, N., Maeda, S., and Takashima, A. (2008) *Curr. Alzheimer Res.* **5,** 591–598
47. Patterson, K. R., Remmers, C., Fu, Y., Brooker, S., Kanaan, N. M., Vana, L., Ward, S., Reyes, J. F., Philibert, K., Glucksman, M. J., and Binder, L. I. (2011) *J. Biol. Chem.* **286,** 23063–23076
48. Sverdlov, M., Shajahan, A. N., and Minshall, R. D. (2007) *J. Cell. Mol. Med.* **11,** 1239–1250
49. Dickey, C. A., Yue, M., Lin, W. L., Dickson, D. W., Dunmore, J. H., Lee, W. C., Zehr, C., West, G., Cao, S., Clark, A. M., Caldwell, G. A., Caldwell, K. A., Eckman, C., Patterson, C., Hutton, M., and Petrucelli, L. (2006) *J. Neurosci.* **26,** 6985–6996
50. Boland, B., Kumar, A., Lee, S., Platt, F. M., Wegiel, J., Yu, W. H., and Nixon, R. A. (2008) *J. Neurosci.* **28,** 6926–6937